PHYSICAL REVIEW E **95**, 010301(R) (2017)

Reconstructing links in directed networks from noisy dynamics

Emily S. C. Ching* and H. C. Tam
Department of Physics, The Chinese University of Hong Kong, Shatin, Hong Kong
(Received 7 March 2016; revised manuscript received 9 August 2016; published 5 January 2017)

We address the long-standing challenge of how to reconstruct links in directed networks from measurements, and present a general method that makes use of a noise-induced relation between network structure and both the time-lagged covariance of measurements taken at two different times and the covariance of measurements taken at the same time. When the coupling functions have certain additional properties, we can further reconstruct the weights of the links.

DOI: 10.1103/PhysRevE.95.010301

The study of networks [1–3] has emerged in many branches of science. Many systems of interest consist of a large number of components that interact with each other. These systems can be represented as networks with the individual components being the nodes or vertices and the interactions between two nodes being the links or edges that join the nodes. The network structure depicting how the nodes are linked is a crucial piece of information for us to understand the behavior and function of the system that the network represents. It is often difficult to directly measure the network structure while the dynamics of individual nodes can be measured with relative ease. This leads to the interesting question of how to reconstruct the links of a network from the measurements of the nodes. For most systems of interest, a node can affect the dynamics of another node but its own dynamics is unaffected by the latter. These systems are represented as directed networks with directional links. In general, the strength of interaction can be different so the links have different weights.

Most existing reconstruction methods apply only for undirected networks in which interactions between two nodes are mutual. A commonly employed idea is to infer links from correlation of measurements, with a larger correlation coefficient interpreted as a higher probability of a link [4,5]. For undirected networks with certain forms of diffusive coupling, it has been shown [6–8] that information of the network structure is contained in a quantity related to the inverse of the covariance matrix. This shows that the common practice of inferring links from correlation would be prone to give erroneous results and also explains why systems can be strongly coupled but have weak pairwise correlation [9]. Other reconstruction methods either assume the dynamics to be linear [10,11] or require additional information such as knowledge about the functional form of the nodal dynamics [12–17] and response dynamics to specific perturbations [18]. A number of techniques have been proposed for the detection of directional coupling from time series measurements but these techniques have limitations [19,20]. Reconstructing links of directed networks from measurements remains a big challenge [21,22].

In this Rapid Communication, we present a general method that reconstructs links in a directed network subject to noise using time-series measurements of the nodes only. We present a noise-induced relation and show how information of the network structure can be extracted using this relation. When the coupling functions have certain additional properties, we can further reconstruct the weights or relative coupling strength of the links.

We study a directed network of N nodes and each node is described by a state variable $x_i(t)$, $i = 1,2,\ldots,N$. The dynamics of the nodes are governed by

$$\frac{dx_i}{dt} = f_i(x_i) + \sum_{j\neq i} g_{ij}A_{ij}h(x_i,x_j) + \eta_i, \tag{1}$$

where f_i describes the intrinsic dynamics of node i and A_{ij} are the elements of the adjacency matrix $\mathbf{A}$. When the dynamics of node i is affected by node j via the coupling function $h(x_i,x_j)$ with strength g_{ij}, $A_{ij} = 1$ and a link joins node j to node i. Otherwise $A_{ij} = g_{ij} = 0$. A_{ij} and g_{ij} are generally asymmetric. The coupling function $h(x,y)$ satisfies $\partial h(x,y)/\partial y > 0$, thus excitatory and inhibitory links have $g_{ij} > 0$ and $g_{ij} < 0$, respectively. We assume no self-interaction such that $A_{ii} \equiv 0$. We model external disturbance acting on node i by a Gaussian white noise η_i of zero mean with $\overline{\eta_i(t)\eta_j(t')} = D_{ij}\delta(t-t')$. $\overline{\cdots}$ denotes an ensemble average over different realizations of the noise.

Our approach is to obtain a mathematical relation between the network structure and quantities that can be measured using only $x_i(t)$ and develop a method of reconstruction based on such mathematical relation. We focus on systems that have stationary fluctuations about a noise-free steady state. This type of dynamics is common and can be found in a class of models of genetic and biochemical networks [23,24] when noise is added. We linearize Eq. (1) around the noise-free solution to obtain

$$\frac{d}{dt}\delta\mathbf{x} \approx \mathbf{Q}\delta\mathbf{x} + \eta, \tag{2}$$

where $\eta = (\eta_1,\ldots,\eta_N)^T$, $\delta\mathbf{x} = (\delta x_1,\ldots,\delta x_N)^T$, and $\delta x_i(t) = x_i(t) - X_i$ is the deviation of the state variable from the noise-free solution X_i. The superscript T denotes a transpose and the matrix $\mathbf{Q}$, with elements

$$Q_{ij} = g_{ij}A_{ij}\left.\frac{\partial h(x,y)}{\partial y}\right|_{x=X_i,y=X_j} + \left[\sum_{k\neq i} g_{ik}A_{ik}\left.\frac{\partial h(x,y)}{\partial x}\right|_{x=X_i,y=X_k} + f_i'(X_i)\right]\delta_{ij}, \tag{3}$$

*ching@phy.cuhk.edu.hk

contains information of the network structure. We define $\mathbf{B}(t_1,t_2)$ by

$$\mathbf{B}(t_1,t_2) \equiv \overline{[\mathbf{x}(t_1)-\overline{\mathbf{x}(t_1)}][\mathbf{x}(t_2)-\overline{\mathbf{x}(t_2)}]^T} = \overline{[\delta\mathbf{x}(t_1)-\overline{\delta\mathbf{x}(t_1)}][\delta\mathbf{x}(t_2)-\overline{\delta\mathbf{x}(t_2)}]^T}. \quad (4)$$

The last equality follows because $\overline{X_i} = X_i$. $B_{ij}(t_1,t_2)$ is the covariance of measurements of node i at t_1 and measurements of node j at time t_2.

Solving Eq. (2), we obtain [25] for $\tau \geqslant 0$

$$\mathbf{B}(t+\tau,t) \approx \exp[(t+\tau)\mathbf{Q}]\mathbf{B}(0,0)\exp(t\mathbf{Q}^T) + \exp(\tau\mathbf{Q})\int_0^t \exp(t'\mathbf{Q})\mathbf{D}\exp(t'\mathbf{Q}^T)dt' \quad (5)$$

which implies

$$\mathbf{B}(t+\tau,t) \approx \exp(\tau\mathbf{Q})\mathbf{B}(t,t). \quad (6)$$

Here, $\mathbf{D}$ is the matrix with elements D_{ij} from the correlation of the noise. Equations (5) and (6) are exact for the linearized system [Eq. (2) with the approximation replaced by an equal sign] and a good approximation for the original nonlinear network [governed by Eq. (1)] in the weak-noise limit. As the system has stationary dynamics, $\mathbf{B}(t,t)$ is independent of t, and $\mathbf{B}(t+\tau,t)$ depends on τ only and can be approximated by long time average:

$$\mathbf{B}(t+\tau,t) \approx \mathbf{K}_\tau \equiv \langle[\mathbf{x}(t+\tau)-\langle\mathbf{x}(t+\tau)\rangle][\mathbf{x}(t)-\langle\mathbf{x}(t)\rangle]^T\rangle, \quad (7)$$

where $\langle\cdots\rangle$ denotes a time average. Thus we have

$$\exp(\tau\mathbf{Q}) \approx \mathbf{K}_\tau\mathbf{K_0}^{-1}. \quad (8)$$

We assume that the N nodes have linearly independent fluctuations so that $\mathbf{K_0}$ is nonsingular. For undirected networks with coupling such that $\mathbf{Q}$ is symmetric and $D_{ij} = \sigma^2\delta_{ij}$, evaluating Eq. (5) at $\tau = 0$ and $t \to \infty$ gives $\mathbf{K_0} \approx \mathbf{B}(t,t) \approx -(\sigma^2/2)\mathbf{Q}^{-1}$, which is a noise-induced relation between the network structure and the inverse of the covariance matrix [6–8]. Equation (8) is an extension of such kind of mathematical relation between network structure and measurements to directed networks. $\mathbf{K_0}$ and $\mathbf{K}_\tau$ can be calculated from the time series measurements of $x_i(t)$. For τ such that $\tau \max_i |\mathrm{Im}(\lambda_i)| < \pi$, where $\mathrm{Im}(\lambda_i)$ is the imaginary part of the eigenvalue λ_i of $\mathbf{Q}$, it can be proved [26] that $\log[\exp(\tau\mathbf{Q})]$ is equal to $\tau\mathbf{Q}$, where log denotes the principal logarithm. Thus for such values of τ, $\mathbf{M} = \log(\mathbf{K}_\tau\mathbf{K_0}^{-1})/\tau \approx \mathbf{Q}$, and using Eq. (3), we have

$$M_{ij} \approx g_{ij}A_{ij}\left.\frac{\partial h(x,y)}{\partial y}\right|_{x=X_i,y=X_j}, \qquad i \neq j. \quad (9)$$

Therefore, the off-diagonal elements of $\mathbf{M}$ separate into different groups depending on whether $A_{ij} = 0$ or $A_{ij} = 1$. We identify these different groups of M_{ij} by clustering using a Gaussian mixture model [27] and, as a result, reconstruct the links of the network. The relevance of Eq. (8) for network reconstruction has been noted independently by Prill *et al.* and Lüsmann [28,29]. Prill *et al.* [28] did not pursue this method but focused on exploring the possibility of extracting connectivity information using only the covariance matrix $\mathbf{K_0}$, whereas Lüsmann [29] studied only networks with linear dynamics.

TABLE I. The networks studied. N_B and N_U are, respectively, the number of bidirectionally and unidirectionally linked pairs of nodes. The number of links N_L is given by $2N_B + N_U$ and the link density ρ is equal to $N_L/[N(N-1)]$.

Network	N	N_B	N_U	N_L	ρ	g_{ij}
DWR1	100	186	1678	2050	0.207	$N(10,2)$
DWR1s	100	186	1678	2050	0.207	$N(10,10)$
DWR2	100	0	1035	1035	0.105	$N(10,2)$
DWSF	1000	3120	3730	9970	0.00998	$P(g_{ij}) \sim g_{ij}^{-6.6}$

We test our method using directed and weighted random (DWR) and directed and weighted scale-free (DWSF) networks (see Table I). DWR1 and DWR2 are directed random networks of connection probability 0.2 with DWR2 further restricted to contain only unidirectional links such that $A_{ij} = 0$ for $i > j$. For both DWR1 and DWR2, g_{ij}'s are taken from a Gaussian distribution $N(10,2)$ of mean 10 and standard deviation 2 and all the links turn out to have $g_{ij} > 0$. DWR1s has the same adjacency matrix A as DWR1 but g_{ij}'s are taken from a different Gaussian distribution $N(10,10)$ such that the links have both positive and negative g_{ij}. DWSF is constructed by converting some bidirectional links of an undirected weighted scale-free network [30] into directional links with the power-law distribution of g_{ij} kept intact and the out-degree $k_{\mathrm{out}}(i) = \sum_j A_{ij}$ distribution being the same as the original power-law degree distribution. We consider nonlinear logistic function

$$f_i(x) = r_i x(1-x) \quad (10)$$

with parameters r_i, and two coupling functions

$$h^{\mathrm{diff}}(x,y) = y - x, \quad (11)$$

$$h^{\mathrm{syn}}(x,y) = (1/\beta_1)\{1+\tanh[\beta_2(y-y_0)]\}. \quad (12)$$

The linear diffusive coupling function h^{diff} is a common model for gap junction coupling while the nonlinear h^{syn} is a generalization [8] of a model [31] for synaptic coupling between neurons. The parameters β_1, β_2, and y_0 are chosen such that the steady-state values X_i are close to y_0. We integrate the equations of motion using the Euler-Maruyama method to obtain $x_i(t)$, recording the time series with a sampling interval δt, then calculate $\mathbf{K}_\tau$ with $\tau = \delta t$ and $\mathbf{K_0}^{-1}$ with a time average over N_{data} data points. We take $D_{ij} = \sigma_i^2\delta_{ij}$ with $\sigma_i = 1$, $\delta t = 5\times10^{-4}$, and $N_{\mathrm{data}} = 2\times10^6$ unless otherwise stated.

We compare the off-diagonal elements of $\mathbf{M}$ and $\mathbf{Q}$ in Fig. 1; the data points scatter around the line $y = x$ confirming Eq. (9). One cause for the data scatter is due to the finite sample size, and the data scatter is reduced when N_{data} is increased [see Fig. 1(d)]. The accuracy of our method increases with N_{data} too (see case 9 of Table II). It is common to measure the accuracy of a method by its sensitivity and specificity, which give, respectively, the relative errors in the prediction of links and nonexistent links of a network. However, for sparse networks with link density $\rho = N_L/[N(N-1)] \ll 1$ (N_L is the number of links), the number of incorrectly inferred links can be substantial leading to a greatly distorted reconstructed

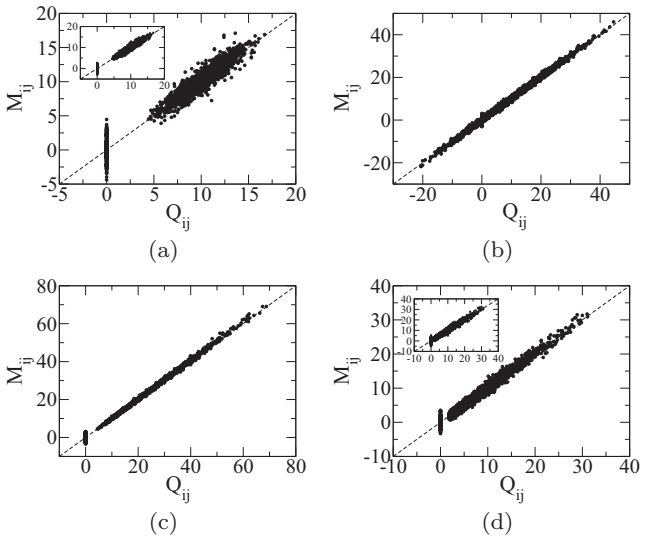

FIG. 1. Verification of $M_{ij} = Q_{ij} = g_{ij}A_{ij}h_y(X_i, X_j)$ for $i \neq j$. (a) Case 2 with nonuniform noise and case 3 with inhomogeneous f_i (inset), (b) case 5 with both excitatory and inhibitory links, (c) case 7, and (d) case 9 with $N_{\text{data}} = 4 \times 10^6$ and $N_{\text{data}} = 2 \times 10^6$ (inset). See Table II for detailed descriptions of the different cases. Dashed line is $y = x$.

network even when the specificity is close to 1. So, we measure the accuracy instead by the error rates FN/N_L and FP/N_L, which are, respectively, the proportion of the links that are missed (false negatives, FN) and the ratio of incorrectly inferred links (false positives, FP) to the number of links (see Table II). Sensitivity is given by $1 - \text{FN}/N_L$, while specificity is given by $1 - (\text{FP}/N_L)\rho/(1-\rho)$. The two error rates are less than 10% for all the cases studied (for case 9, the error rates are lowered to less than 10% with a larger $N_{\text{data}} = 4 \times 10^6$),

TABLE II. Accuracy of our reconstruction as measured by the error rates FN/N_L and FP/N_L (in %) for the cases studied. Case 2: σ_i taken from $N(1,0.2)$. Case 3: r_i taken from a uniform distribution $U(1,50)$ from 1 to 50. Case 4: $(\beta_1,\beta_2,y_0) = (2,0.5,4)$. Case 7: $(\beta_1,\beta_2,y_0) = (0.1,0.5,4)$. Case 9: $(\beta_1,\beta_2,y_0) = (0.5,0.5,4)$ and $N_{\text{data}} = 4 \times 10^6$ (results for $N_{\text{data}} = 2 \times 10^6$ are given in parentheses). Case (ii): $(\beta_1,\beta_2,y_0) = (20,1,1)$. e_G is the average percentage error of the reconstructed relative coupling strength $\hat{G}_{ij}$ or $\hat{G}_j^{\text{out}}(i)$ excluding missed and incorrectly predicted links.

Case	Network	Dynamics	FN/N_L	FP/N_L	e_G
1	DWR1	$r_i = 10$; h^{diff}	0	0	5.7
2	DWR1	$r_i = 10$; Gaussian σ_i; h^{diff}	0	0.63	6.0
3	DWR1	uniform r_i; h^{diff}	0	0	6.0
4	DWR1	$r_i = 10$; h^{syn}	2.98	2.00	14.2
5	DWR1s	$r_i = 10$; h^{diff}	9.32	1.90	9.8
6	DWR2	$r_i = 50$; h^{diff}	0	0	4.3
7	DWR2	$r_i = 50$; h^{syn}	0	3.38	4.5
8	DWSF	$r_i = 100$; h^{diff}	0.50	1.11	6.9
9	DWSF	$r_i = 100$; h^{syn}	0.65 (9.20)	2.84 (21.60)	10.3 (13.1)
(i)	DWR1	$f_i = 0$; h^{cubic}	4.24	2.78	16.6
(ii)	DWR1	Rössler; h^{syn}	1.90	1.17	14.5

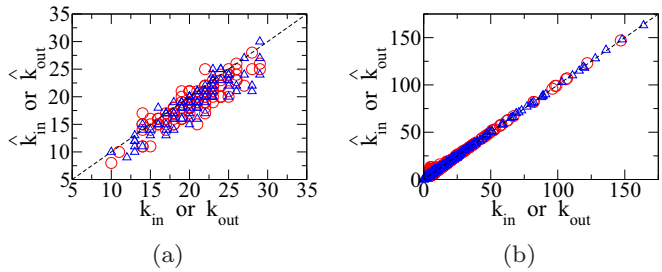

FIG. 2. Comparison of the reconstructed in degrees $\hat{k}_{\text{in}}$ (triangles) and out degrees $\hat{k}_{\text{out}}$ (circles) with the actual values for (a) case 5 and (b) case 9 with $N_{\text{data}} = 4 \times 10^6$.

including network acted upon by nonuniform noise (case 2), network with inhomogeneous intrinsic dynamics (case 3), and network with both excitatory and inhibitory links (case 5). From Eq. (9), we expect that weak links with small $|g_{ij}|$ are difficult to detect. Indeed all links that are missed are of relatively weak coupling strength. For cases 5 and 9 that have the highest error rates in DWR and DWSF networks, respectively, we compare directly the reconstructed in- and out-degree of the nodes, $\hat{k}_{\text{in}}$ and $\hat{k}_{\text{out}}$, with the actual values in Fig. 2. Good agreement is found and our method can capture the power-law out-degree distribution of DWSF.

We define the relative coupling strength of an incoming and outgoing link of node i from and to node j by

$$G_j^{\text{in}}(i) \equiv \frac{g_{ij}}{\langle g\rangle_{\text{in}}(i)}; \qquad G_j^{\text{out}}(i) \equiv \frac{g_{ji}}{\langle g\rangle_{\text{out}}(i)}, \tag{13}$$

respectively, where $\langle g\rangle_{\text{in}}(i) \equiv \sum_j |g_{ij}|A_{ij}/k_{\text{in}}(i)$ and $\langle g\rangle_{\text{out}}(i) \equiv \sum_j |g_{ji}|A_{ji}/k_{\text{out}}(i)$ are the average (absolute) coupling strength of the incoming or outgoing links of node i. If $\partial h(x,y)/\partial y$ depends on y only as for h^{syn},

$$G_j^{\text{out}}(i) \approx \frac{M_{ji}\hat{k}_{\text{out}}(i)}{\sum_{k\leftarrow i}|M_{ki}|} \equiv \hat{G}_j^{\text{out}}(i). \tag{14}$$

$\sum_{k\leftarrow i}$ represents a sum over nodes k that are reconstructed to be linked from node i. Similarly if $\partial h(x,y)/\partial y$ depends on x only, we can reconstruct $G_j^{\text{in}}(i)$ using $\hat{G}_j^{\text{in}}(i) \equiv M_{ij}\hat{k}_{\text{in}}(i)/\sum_{k\rightarrow i}|M_{ik}|$, where $\sum_{k\rightarrow i}$ represents a sum over nodes k that are reconstructed to link to node i. If $\partial h(x,y)/\partial y$ is a constant as for h^{diff},

$$G_{ij} \equiv \frac{g_{ij}}{\langle g\rangle} \approx \frac{M_{ij}\hat{k}_{\text{tot}}}{\sum_{n,l\leftrightarrow n}|M_{nl}|} \equiv \hat{G}_{ij}, \tag{15}$$

where $\langle g\rangle \equiv \sum_{ij}|g_{ij}|A_{ij}/\sum_{ij}A_{ij}$ and $\hat{k}_{\text{tot}} = \sum_i \hat{k}_{\text{in}}(i) = \sum_i \hat{k}_{\text{out}}(i)$. In Fig. 3, we compare the reconstructed relative coupling strength $\hat{G}_{ij}$ and $\hat{G}_j^{\text{out}}(i)$ with the actual values. The average percentage error e_G (excluding missed and incorrectly predicted links) ranges between 4.3% and 14.2% for cases 1–9 (see Table II).

In [32], the authors focused on the linearized dynamics Eq. (2) and obtained a relation between $\mathbf{Q}$ and the "velocity-variable" covariance matrix of dx_i/dt and $x_j(t)$ and the covariance matrix. Their relation is the $\tau \rightarrow 0$ limit of Eq. (8). Their relation with dx_i/dt approximated as $[x_i(t+\tau) - x_i(t)]/\tau$ (recall τ is equal to the sampling interval δt) is equivalent

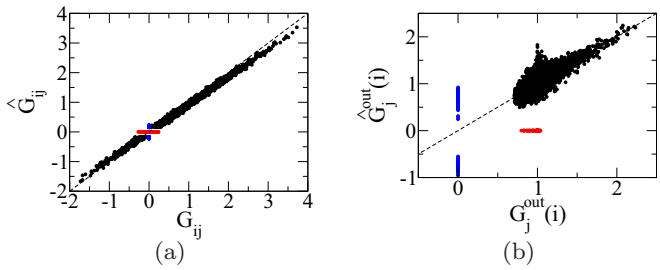

FIG. 3. Comparison of reconstructed $\hat{G}_{ij}$ and $\hat{G}_j^{\text{out}}(i)$ with the actual values for (a) case 5 and (b) case 9 with $N_{\text{data}} = 4 \times 10^6$. Missed links (red) have $G_{ij} \neq 0$ $[G_j^{\text{out}}(i) \neq 0]$ but $\hat{G}_{ij} = 0$ $[\hat{G}_j^{\text{out}}(i) = 0]$, while incorrectly inferred links (blue) have $G_{ij} = 0$ $[G_j^{\text{out}}(i) = 0]$ but $\hat{G}_{ij} \neq 0$ $[\hat{G}_j^{\text{out}}(i) \neq 0]$. Dashed line is $y = x$.

to the approximation

$$\mathbf{M} \approx [\mathbf{K}_\tau \mathbf{K_0}^{-1} - \mathbf{I}]/\tau, \tag{16}$$

where $\mathbf{I}$ is the identity matrix. This approximation is good only when τ is sufficiently small such that $\exp(\tau\mathbf{Q}) \approx \mathbf{I} + \tau\mathbf{Q}$. In Table III, we compare the error rates of the reconstruction results using our method and the approximation Eq. (16). One sees clearly that our method gives more accurate reconstruction results, particularly for larger τ.

The theoretical basis of our method is given by Eq. (6), which holds for systems that have stationary fluctuations about a noise-free steady state in the weak noise limit with the linearized dynamics described by Eq. (2). To investigate the general applicability of our method, we consider two additional cases: (i) $f_i = 0$ and $h^{\text{cubic}}(x,y) = (y-x)^3$ and (ii) nodes of three-dimensional state variables $(x_i(t), y_i(t), z_i(t))$ described by the nonlinear Rössler dynamics [33]:

$$\dot{x}_i = -y_i - z_i + \sum_{j \neq i} g_{ij} A_{ij} h(x_i, x_j) + \eta_i, \tag{17}$$

$$\dot{y}_i = x_i + a y_i. \tag{18}$$

$$\dot{z}_i = b + z_i(x_i - c) \tag{19}$$

TABLE III. Comparison of the error rates of the reconstruction results of case 1 using our method and the approximation Eq. (16) based on [32]. Error rates for the latter are given in parentheses. $N_{\text{data}} = 10^6$ for calculating $\mathbf{K}_\tau$ and $\mathbf{K_0}$.

$\tau = \delta t$	FN/N_L (%)	FP/N_L (%)	e_G (%)
1×10^{-3}	0 (0)	0 (0)	6.2 (6.4)
5×10^{-3}	0 (0)	0 (0.15)	4.7 (11.5)
1×10^{-2}	0 (2.44)	0.68 (9.66)	8.2 (20.0)

with $a = b = 0.2$ and $c = 9$. In case (i), the noise-free steady state is node independent, thus $Q_{ij} = 0$ for $i \neq j$, which implies that the dynamics of fluctuations are intrinsically nonlinear. In case (ii), the system does not approach a steady state in the absence of noise and have chaotic dynamics when the nodes are decoupled. For these additional cases, we find that $M_{ij} \approx C g_{ij} A_{ij}$ for $i \neq j$ for some constant C, which implies Eq. (15) should also hold. Error rates for these additional cases are low (see Table II). Hence we have numerical evidence that our method is applicable for systems for which the derivation of Eq. (6) does not directly apply.

In conclusion, we have presented a method that reconstructs links in directed networks with noisy nonlinear dynamics using only time series measurements of the nodes. Our method is based on a noise-induced mathematical relation Eq. (6) or Eq. (8). When the coupling functions have certain additional properties, our method can further reconstruct the weights of the links. Using numerically simulated data, we have shown that our method can successfully reconstruct the network structure with low error rates for directed weighted random and directed weighted scale-free networks with nonlinear dynamics and coupling functions.

We acknowledge the Hong Kong Research Grants Council (Grant No. CUHK 14300914) for support, and thank K. C. Lin for introducing us to clustering analysis using Gaussian mixture models in MATLAB.

[1] S. H. Strogatz, Exploring complex networks, Nature (London) **410**, 268 (2001).

[2] R. Albert and A.-L. Barabási, Statistical mechanics of complex networks, Rev. Mod. Phys. **74**, 47 (2002).

[3] M. E. J. Newman, The structure and function of complex networks, SIAM Rev. **45**, 167 (2003).

[4] J. M. Stuart, E. Segal, D. Koller, and S. K. Jim, A gene-coexpression network for global discovery of conserved genetic modules, Science **302**, 249 (2003).

[5] V. M. Eguíluz, D. R. Chialvo, G. A. Cecchi, M. Baliki, and A. V. Apkarian, Scale-Free Brain Functional Networks, Phys. Rev. Lett. **94**, 018102 (2005).

[6] J. Ren, W.-X. Wang, B. Li, and Y.-C. Lai, Noise Bridges Dynamical Correlation and Topology in Coupled Oscillator Networks, Phys. Rev. Lett. **104**, 058701 (2010).

[7] E. S. C. Ching, P. Y. Lai, and C. Y. Leung, Extracting connectivity from dynamics of networks with uniform bidirectional coupling, Phys. Rev. E **88**, 042817 (2013); Erratum: Extracting connectivity from dynamics of networks with uniform bidirectional coupling [Phys. Rev. E **88**, 042817 (2013)], **89**, 029901(E) (2014).

[8] E. S. C. Ching, P. Y. Lai, and C. Y. Leung, Reconstructing weighted networks from dynamics, Phys. Rev. E **91**, 030801(R) (2015).

[9] E. Schneidman, M. J. Berry, R. Segev, and W. Bialek, Weak pairwise correlations imply strongly correlated network states in a neural population, Nature (London) **440**, 1007 (2006).

[10] M. K. S. Yeung, J. Tegnér, and J. J. Collins, Reverse engineering gene networks using singular value decomposition and robust regression, Proc. Natl. Acad. Sci. USA **99**, 6163 (2002).

[11] D. Napoletani and T. D. Sauer, Reconstructing the topology of sparsely connected dynamical networks, Phys. Rev. E **77**, 026103 (2008).

[12] D. Yu, M. Righero, and L. Kocarev, Estimating Topology of Networks, Phys. Rev. Lett. **97**, 188701 (2006).

[13] S. G. Shandilya and M. Timme, Inferring network topolgy from complex dynamics, New J. Phys. **13**, 013004 (2011).

[14] Z. Levnajić and A. Pikovsky, Network Reconstruction from Random Phase Resetting, Phys. Rev. Lett. **107**, 034101 (2011).

[15] S. Shahrampour and V. M. Preciado, Reconstruction of directed networks from consensus dynamics, in *Proceedings of the American Control Conference (ACC)* (IEEE, 2013), pp. 1685–1690.

[16] Z. Levnajić and A. Pikovsky, Untangling complex dynamical systems via derivative-variable correlations, Sci. Rep. **4**, 5030 (2014).

[17] A. Pikovsky, Reconstruction of a neural network from a time series of firing rates, Phys. Rev. E **93**, 062313 (2016).

[18] M. Timme, Revealing Network Connectivity from Response Dynamics, Phys. Rev. Lett. **98**, 224101 (2007).

[19] D. Smirnov and R. G. Andrzejak, Detection of weak directional coupling: Phase-dynamics approach versus state-space approach, Phys. Rev. E **71**, 036207 (2005).

[20] D. Smirnov, B. Schelter, N. Winterhalder, and J. Timmer, Revealing direction of coupling between neuronal oscillators from time series: Phase dynamics modeling versus partial directed coherence, Chaos **17**, 013111 (2007).

[21] M. Timme, Does dynamics reflect topology in directed networks?, Europhys. Lett. **76**, 367 (2006).

[22] M. Timme and J. Casadiego, Revealing networks from dynamics: An introduction, J. Phys. A: Math. Theor. **47**, 343001 (2014).

[23] T.-C. Ni and M. A. Savageau, Application of biochemical systems theory to metabolism in human red blood cells, J. Biol. Chem. **271**, 7927 (1996).

[24] E. O. Voit and T. Radivoyevitch, Biochemical systems analysis of genome-wide expression data, Bioinformatics **16**, 1023 (2000).

[25] L. Arnold, *Stochastic Differential Equations: Theory and Applications* (Wiley-Interscience, New York, 1974).

[26] Using Theorem 1.31 of N. J. Higham, *Functions of Matrices: Theory and Computation* (SIAM, Philadelphia, 2008), we can show that $\log[\exp(\tau\mathbf{Q})] = \tau\mathbf{Q}$ when τ satisfies the condition $\tau \max_i |\mathrm{Im}(\lambda_i)| < \pi$ for eigenvalues λ_i's of $\mathbf{Q}$.

[27] We use MATLAB fitgmdist to fit the M_{ij} data by a Gaussian mixture model of two components, then use MATLAB cluster to obtain the posterior probabilities of each component for each data point. For each data point M_{ij}, if the posterior probability of belonging to the component with a mean closest to 0 (which is associated with the component for $A_{ij} = 0$) is less than 0.5, then this M_{ij} is inferred to be from connected nodes and $\hat{A}_{ij} = 1$. Otherwise, $\hat{A}_{ij} = 0$. For DWR networks, clustering analysis is performed on all M_{ij} $(i \neq j)$ values as a whole, while for the DWSF network, clustering analysis is performed on M_{ij} values for fixed j separately for each j.

[28] R. J. Prill, R. Vogel, G. A. Cecchi, G. Altan-Bonnet, and G. Stolovitzky, Noise-driven causal inference in biomolecular networks, PLoS One **10**, e0125777 (2015).

[29] B. J. Lüsmann, Reconstruction of physical interactions in stationary stochastic network dynamics, Master thesis, Max Planck Institute for Dynamics and Self-Organization, 2015.

[30] A. Barrat, M. Barthélemy, and A. Vespignani, Weighted Evolving Networks: Coupling Topology and Weight Dynamics, Phys. Rev. Lett. **92**, 228701 (2004).

[31] G. B. Ermentrout and N. Kopell, Oscillator death in systems of coupled neural oscillators, SIAM J. Appl. Math. **50**, 125 (1990).

[32] Z. Zhang, Z. Zheng, H. Niu, Y. Mi, S. Wu, and G. Hu, Solving the inverse problem of noise-driven dynamic networks, Phys. Rev. E **91**, 012814 (2015).

[33] O. E. Rössler, An equation for continuous chaos, Phys. Lett. A **57**, 397 (1976).